

Radial Distribution Function Analysis Study on Alkali and Heat-Treated Ramie Fiber

K. P. SAO,* B. K. SAMANTARAY, and S. BHATTACHERJEE

Department of Physics and Meteorology, Indian Institute of Technology, Kharagpur 721302, India

SYNOPSIS

The radial distribution function (RDF) analysis of wide-angle X-ray diffraction by ramie fibers in untreated condition and after treatment with alkali of mercerizing strength or heat have been carried out. Interatomic distances, coordination numbers, mean square displacements, and coupling constants for different atom pairs have been calculated. The results have been interpreted in terms of a difference in both the conformation and packing of molecular chains in raw and alkali-treated ramie. In general, the coupling constant values have been found to be more in alkali-treated ramie, indicating relatively weak bond strength. Heat-treated ramie shows a marginal decrease in coupling constant values. © 1994 John Wiley & Sons, Inc.

INTRODUCTION

Cellulose, a naturally occurring polymer is known to consist of D-anhydroglucopyranose units joined together by β -1, 4-glycosidic bonds. In the semicrystalline ramie fiber, it is generally considered that the cellulose chains are arranged in crystalline (ordered) and amorphous (disordered) regions.¹ The interesting feature of cellulose crystalline structure is its ability to exist in different crystallographic polymorphs such as cellulose I, II, etc. Hence for a detailed characterization of the supermolecular structure of cellulose, both packing and conformation of chain molecules are important. The imperfect crystal structure and disorders in cellulose give rise to an X-ray diffraction pattern with high background and broadened peaks. It is well established² that the X-ray pattern from a randomly oriented system is spherically symmetrical and can be mathematically transformed into a radial distribution function that specifies the atomic or electronic density as a function of the distance from every atom or electron in the system regarded successively as the origin. This serves as a powerful and suitable tool for structural

characterization of nonideal semicrystalline systems such as the present one under study.

Attempts have been made by several workers³⁻¹⁰ to apply the radial distribution function (RDF) analysis of X-ray diffraction data to cellulose. Bjørnhaug et al.^{3,4} and Ellefsen et al.^{5,6} observed that the main features of RDF curves of cellulose appear to be related to the lateral packing of the molecules, whereas the smaller ripples are connected to intratomic distances along and within a single chain. They concluded that the RDF of amorphous cellulose essentially depends on the spatial arrangement of successive anhydroglucose units in the chain molecule, and there is an irregular packing of rods of a diameter of about 0.5 nm. Heyn⁷ studied the RDF of jute and rayon from the X-ray scattering at small angle and obtained different distribution curves with different fibers and under different conditions of swelling. Norman,⁸ considering cylindrical symmetry, interpreted the results of X-ray diffraction from oriented fibers of ramie (cellulose I) and Fortisan (cellulose II) in terms of similar conformation. Petitpas⁹ concluded that cellulose I and cellulose II possess different chain conformation. Fink et al.¹⁰ compared the experimental results of amorphous cellulose samples prepared by ball milling of cellulose I and II and by saponification of cellulose triacetate with model calculations. They found that at small distances ($r < 0.5$ nm) experimentally ob-

* To whom correspondence should be addressed.

Present address: Physics Division, JTRIL (ICAR), 12, Regent Park, Calcutta 700 040, India.

Journal of Applied Polymer Science, Vol. 52, 1917-1923 (1994)

© 1994 John Wiley & Sons, Inc.

CCC 0021-8995/94/131917-07

tained RDFs are in rather good agreement with RDFs from a model with bent and twisted backbone conformations.

The present work reports the results of RDF analysis of wide-angle X-ray diffraction by semi-crystalline ramie fibers in untreated condition and after treatments with alkali or heat. The effect of alkali or heat on cellulose structure has attracted considerable attention for various practical reasons in relation to industrial processes and applications.¹¹ The present study forms a part of our effort to apply advanced X-ray diffraction methods for the characterization of poorly crystalline natural fibers.

EXPERIMENTAL

Sample Preparation

Degummed (2–3% gum content) and mild bleached ramie fibers¹² were suitably combed and cut to about 10 cm length. These were treated with aqueous NaOH solutions of mercerizing strength [18% (w/w) at room temperature ($\sim 30^\circ\text{C}$) and 12% (w/w) at 0°C , respectively] for 1 h. After treatment the fibers were washed free of alkali with distilled water, scoured with dilute acetic acid and finally washed free of acid with water and then air-dried. To obtain alkali-cellulose complex, the fibers, after treatment with 18% NaOH solution at room temperature (RT) were carefully pressed to remove excess of alkali and then air-dried without washing. It is known¹³ that at the above concentration of alkali, soda cellulose I is formed, which on drying gives soda cellulose III characterized by $\text{C}_6\text{H}_{10}\text{O}_5$, NaOH, $2\text{H}_2\text{O}$. The similarity of unit cell parameters of Na-cellulose I and III suggests that only marginal changes in crystalline packing and other structural features occur during such transformation.¹⁴

The fibers were also heat-treated for 1 h each at 250°C and 300°C , respectively, in an electric muffle furnace fitted with temperature control. Thermogravimetric (TG) and differential thermal analysis (DTA) showed that the major weight loss and degradation in ramie occurs only above 300°C . After treatment the samples were slowly cooled down to room temperature. The above fiber samples were then finely powdered for X-ray study.

Measurement of X-ray Intensity

The experimental data were obtained for the above finely powdered and randomized samples in the range $S = 4\pi \sin \theta/\lambda \sim 4\text{--}70 \text{ nm}^{-1}$ with the help of

a Phillips X-ray diffractometer (PW 1710) using monochromatized (Ni-filtered) $\text{CuK}\alpha$ X-ray radiation at 40 kV and 20 mA. To minimize the effect of preferred orientation, the mean of several runs was taken for a sample.

Calculation of Radial Distribution Function

The experimental intensities were first suitably corrected for background, polarization, and absorption following the procedure described by Kruh.¹⁵ Tabulated values of atomic scattering factor¹⁶ and incoherent scattering factor¹⁷ were used for obtaining the independent scattering curves. The corrected intensities were scaled to electron units using the technique of Krough-Moe.¹⁸ The corrections were made using the detailed procedure as described by Kruh¹⁵ and Warren.¹⁹ Finally the radial distribution function for the polyatomic system was obtained using the equation¹⁵

$$4\pi r^2 \rho_e(r) = 4\pi r^2 \rho_{0e}(r) + \frac{2r}{\pi} \int_0^\infty Si(S) M_1(S) M_2(S) M_3(S) \sin Sr dS \quad (1)$$

The differential RDF (DRDF) is given by

$$4\pi r^2 [\rho_e(r) - \rho_{0e}(r)] = \frac{2r}{\pi} \int_0^\infty Si(S) M_1(S) M_2(S) M_3(S) \sin Sr dS \quad (2)$$

where

$$i(S) = \frac{I}{K} - \left(\sum x_i f_i^2 + \sum x_i I_{\text{inc}} \right) \quad (3)$$

x_i is the mole fraction and f_i is the atomic scattering factor for atom of type i , I is the unscaled intensity, I_{inc} represents the incoherent intensities, and K is the scale factor given by¹⁸

$$K = \frac{\int S^2 I dS}{-2\pi^2 \rho_0 [\sum x_i f_i(0)]^2 + \int S^2 [\sum x_i f_i^2 + I_{\text{inc}}] dS} \quad (4)$$

and $\rho_{0e} = \rho_0 [\sum x_i f_i(0)]^2$, ρ_0 being the average density of atoms in the sample, and subscript e denotes the electron density function. $M_1(S)$ is a sharpening

function given by $\{[\sum x_i f_i(0)]/[\sum x_i f_i(S)]\}^2$. $M_2(S)$ is a temperature or convergence factor given by $\exp(-bS^2)$ while $M_3(S)$ is a step function, which has values one up to $S = S_{\max}$ and zero after that.

The value of b was adjusted till the ripples in the low region were considerably reduced. The value $b = 0.02 \times 10^{-2} \text{ nm}^2$ was found to be satisfactory and used in the present study. For the above calculations, a computer program was written in Fortran and run in a Cyber 180 computer. The overlapped peaks in the RDF curve were resolved by fitting a multiple Gaussian function.²⁰ The coordination numbers were calculated from the area of the resolved peaks.² The mean square displacements and the coupling constants associated with the various interatomic distances were calculated^{20,21} from the half-width of the resolved Gaussian curves. The coupling constant gives an approximate idea of the relative strength of the bond. It is inversely related to the bond strength and increases with a decrease in the bond strength. Its value is unity for a completely uncoupled system while for a completely coupled case it is zero.

RESULTS AND DISCUSSION

Alkali-Treated Ramie

Figure 1 shows the RDF curve of raw and alkali-treated ramie samples. Figure 2 depicts the DRDF curves. Table I gives the peak positions, coordination numbers, mean square displacement of atoms, and coupling constant values.

It is seen from Table I that the coordination number of the nearest neighbor ($\sim 0.14 \text{ nm}$) in raw ramie is about 3, and it increases to about 6 for the second nearest neighbor ($\sim 0.25 \text{ nm}$). For the third nearest neighbor ($\sim 0.36 \text{ nm}$) it again decreases to about 2, after which a steady increase in the coordination number with increasing nearest neighbor distance is observed. It is further seen from Table I that in alkali-treated samples the coordination number of the nearest neighbor decreases slightly to around 2, while that of the second nearest neighbor it increases slightly to around 7 for air-dried soda cellulose compared to an untreated sample. A significant increase in coordination number is also found for the fourth nearest neighbor distance. It is also interesting to note that in the mercerized samples the coordination number for the interatomic distance of about 0.5 nm is remarkably less compared to that of untreated samples. It is further seen from Table I that the more the coordination number,

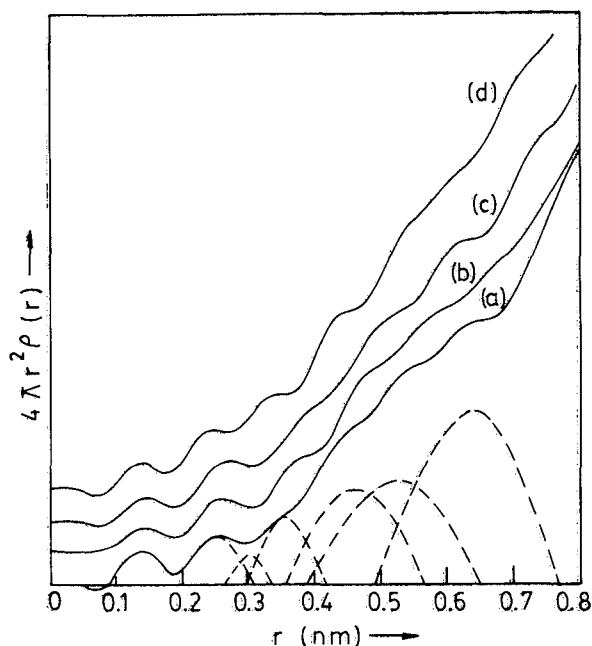


Figure 1 Radial distribution function curves for alkali-treated ramie: (a) untreated, (b) 18% NaOH at RT, (c) 12% NaOH at 0°C , and (d) air-dried soda cellulose (18% NaOH at RT).

the more is the coupling constant value associated with the interatomic vector. In general, the coupling constant values corresponding to the different interatomic vectors are more in alkali-treated ramie (higher in air-dried soda cellulose) than the values in the untreated sample. It is also seen (Fig. 2) that the DRDF peaks are well resolved in the alkali-treated samples, and a marked change in peak position and shape compared to raw ramie is observed in the region $0.3\text{--}0.6 \text{ nm}$. The peak position of the first nearest neighbor ($\sim 0.14 \text{ nm}$) is practically the same for all the samples.

Before initiating discussion of the above results, the following points must be considered. First, in a semicrystalline polymer such as cellulose there is no sharp dividing line between the crystalline and the so-called amorphous regions.²² Second, the molecules in cellulose are held together by at least three types of bond, namely, primary valence bonds, van der Waals forces, and hydrogen bonds. Finally in such a system, both intrachain and interchain scattering contribute to RDF. The intrachain peaks occur mainly at low scattering vectors while the contribution of interchain scattering dominates at higher scattering vectors.²³ The intrachain scattering helps to resolve the chain conformation while interchain scattering helps to explore the possible

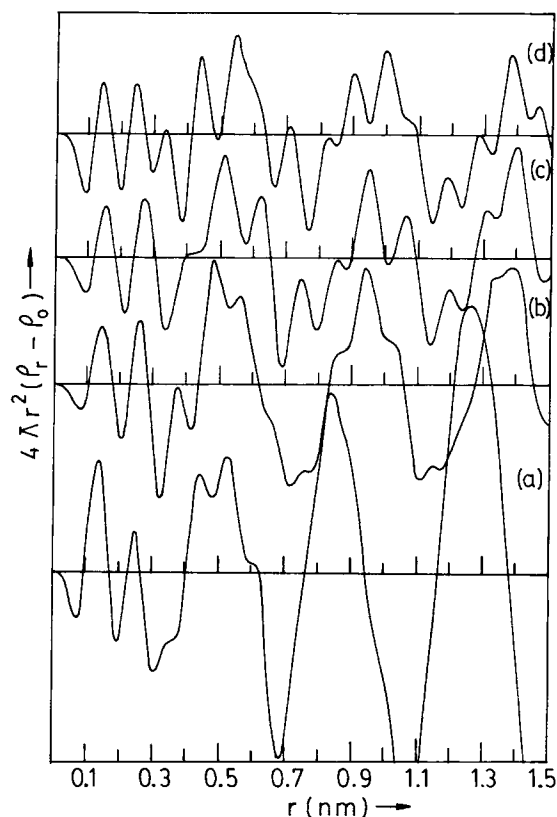


Figure 2 Differential radial distribution curves for alkali-treated ramie: (a) untreated, (b) 18% NaOH at RT, (c) 12% NaOH at 0°C, and (d) air-dried soda cellulose (18% NaOH at RT).

packing arrangement of the chains. It is, however, difficult to achieve a separation in real space of the above two contributions since the Fourier transform of spherically averaged data causes some superposition of intrachain and interchain information.

The first peak near 0.14 nm in the RDF curve corresponds to the nearest neighbor C—C/C—O distance in the glucose molecule.²⁴ The second nearest neighbor C—C/C—O distance contribute to the pronounced maxima at 0.25 nm. This also corresponds to the separation of glucose rings in the hydrogen bonded (020) plane of cellulose lattice. The third nearest neighbor distance of about 0.3 nm also corresponds to the nearest distance of atomic centers if only van der Waals forces holds the lattice.²⁵ It may be mentioned here that the cellulose lattice behaves as a layered structure consisting of sheets of chains held together chiefly by van der Waals forces.^{22,26} For the higher neighbor distances the intermolecular contribution should increase. The maxima near 0.53 nm corresponds to the repeat distance of glucose molecule. The coordination number

as obtained from the RDF are the effective number of atoms in the coordination sphere surrounding the particular type of atom. They result from the weighted contributions of the different constituents and depend on their concentrations and relative values of their scattering factors.²⁷ The variation in coordination number for the first few nearest neighbors in raw ramie seems to be in accordance with the model²⁸ conformation of cellobiose unit. The change in lattice and hydrogen bonding network, increase in distortion and amorphous content on treatment with alkali of mercerizing strength²² will definitely have an effect on the coordination number and coupling constant values associated with different interatomic vectors. The significant increase in coupling constant value corresponding to the interatomic distance of about 0.3 nm most likely indicates the decreased cohesion between the layers or sheets of chains as discussed earlier. In general, the increase in coupling constant or decrease in the relative bond strength in alkali-treated ramie (Table I) indicates the loosening of the structure.

The DRDF curves (Fig. 2) in the region below 0.1 nm should ideally be a straight line with a linear slope of $-4\pi\rho_0$. This ideal situation is, however, difficult to realize in practice, although Wang et al.²³ tried to adjust the experimental DRDF to the theoretically expected values by an iteration procedure. Moreover, in the DRDF curve some variation from that of the RDF curve in respect of resolution and interatomic distance might be expected at large r values due to the multiple Gaussian curve fitting in the case of the latter. The peak position at about 0.14 nm represents the fundamental nearest neighbor distance corresponding to C—C/C—O bond as mentioned earlier. The peak shape and position for $r > 0.2$ nm in the alkali-treated samples show significant variation compared to untreated ramie. As discussed above, the location of the peaks at low scattering vectors depend on the directions of these vectors and give information about the conformation of cellulose chain. In the region 0.3–0.6 nm, as pointed out above, the peaks around 0.35, 0.44, and 0.53 nm of raw ramie shifts slightly to higher r values in the mercerized samples. In raw ramie the peaks above 0.6 nm are not well resolved apart from a intense peak around 0.84 nm, which correspond nearly to edge-on packing distance of two chains.²⁵ This might be due to higher crystallinity and better chain alignment in raw ramie. Differences are also noted in the 0.8–1.0 nm region of mercerized ramie and air-dried soda cellulose complex (Fig. 2). Perhaps the most important of the swelling phenomenon is the action of sodium hydroxide in forming alkali

cellulose. As discussed earlier considering cellulose as a layered structure, swelling causes lateral expansion of these layers of chain molecules. The molecule of swelling reagent may also form a secondary valence bond with the cellulose molecule. Moreover, the nature and extent of the amorphous region also play an important role. Thus, the above results of RDF analysis indicate a change in both conformation and packing of molecular chains in ramie fiber on treatment with alkali of mercerizing strength. This further supports the evidences obtained^{12,29-31} using different physical techniques such as infrared (IR), Raman and nuclear magnetic resonance (NMR) spectroscopy regarding the conformational change in molecular chains during the conversion of cellulose I to cellulose II on alkali treatment.

Heat-Treated Ramie

The RDF curves calculated from the room temperature X-ray diffraction patterns of heat-treated ramie fibers at 250 and at 300°C, respectively, are shown in Figure 3. The peak positions, coordination numbers, and coupling constants associated with different interatomic distances are given in Table II. The DRDF curves are shown in Figure 4.

The peak positions (Table II) in the heat-treated ramie do not show appreciable variation compared to that of raw ramie. However, the coupling constant values, in general, are observed to decrease regularly while the mean square displacements increase with temperature barring one or two cases marginally. The coordination numbers also show slight variation in the sample with temperature. However, in the sample heat-treated at 300°C a sudden sharp drop in the value of coordination number corresponding to the interatomic distance of about 0.45 nm is observed. Further in the DRDF curves (Fig. 4), interesting changes with temperature are observed in the region 0.4–0.6 nm with the emergence of a broad peak around 0.45 nm in the sample heat-treated at 300°C. The shoulder around 0.61 nm in raw fiber develops into a prominent peak in the heat-treated ramie. Compared to the curve for raw ramie, peaks in the region beyond 0.6 nm, tend to resolve for sample heat-treated at 250°C, resulting finally into a large number of well-separated peaks for sample heat-treated at 300°C. Furthermore these well-resolved peaks, however, are found to have achieved resolution at the cost of their intensities, which are much less compared to that of the sample heat-treated at 250°C.

It has been observed²² that the crystallinity and lateral crystallite size in ramie decreases consider-

Table I Peak Position (PP), Coordination Number (CN), Mean Square Displacement (\bar{u}^2), and Coupling Constant (CC) Values in Alkali-Treated Ramie

PP (nm)	Untreated			Air-dried Soda Cellulose (18% NaOH at RT)			Mercerized (18% NaOH at RT)			Mercerized (12% NaOH at 0°C)					
	CN	$\bar{u}^2 \times 10^{-2}$ (nm ²)	CC	PP (nm)	CN	$\bar{u}^2 \times 10^{-2}$ (nm ²)	CC	PP (nm)	CN	$\bar{u}^2 \times 10^{-2}$ (nm ²)	CC	PP (nm)	CN	$\bar{u}^2 \times 10^{-2}$ (nm ²)	CC
0.14	3.5	0.06	0.34	0.14	2.4	0.06	0.50	0.15	2.3	0.06	0.46	0.15	2.4	0.06	0.48
0.25	5.9	0.10	0.42	0.25	7.3	0.12	0.73	0.26	6.6	0.10	0.60	0.27	8.6	0.15	0.74
0.30	2.1	0.03	0.22	0.30	2.0	0.05	0.48	0.31	2.3	0.06	0.54	0.31	1.1	0.06	0.47
0.36	7.8	0.09	0.42	0.34	11.2	0.13	0.75	0.38	12.6	0.13	0.66	0.39	15.5	0.15	0.76
0.46	21.7	0.38	0.83	0.43	18.4	0.27	1.0	0.46	19.2	0.22	0.87	0.48	23.6	0.22	0.92
0.53	27.6	0.53	0.98	0.48	21.4	0.22	1.0	0.51	16.5	0.23	0.88	0.51	9.8	0.11	0.63

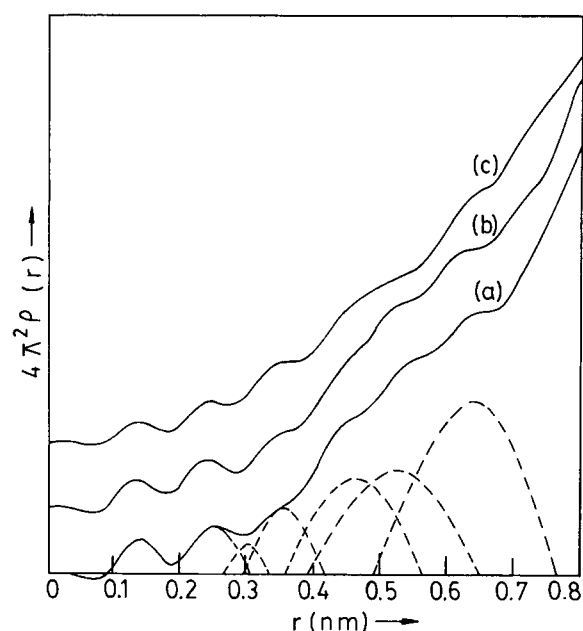


Figure 3 Radial distribution function curves for heat-treated ramie: (a) untreated, (b) 250°C, and (c) 300°C.

ably for sample heat-treated at 250°C while the sample heat-treated at 300°C behaves almost like an amorphous structure showing a broad maxima around $2\theta \sim 24^\circ$ in the X-ray scattering curve. The marginal decrease in coupling constant values is most likely due to dehydration and auto-crosslinking of the anhydroglucose units.³² Also Hatakeyama et al.³³ pointed out the formation of hydrogen bond by free OH groups in amorphous cellulose on heat treatment. The random chain scission at 300°C and even loss of some volatile molecules, which is likely to take place at such high temperature, may contribute to the marked decrease in coordination number observed at 0.45 nm. The change in features of the DRDF curves in the region 0.4–0.6 nm noted

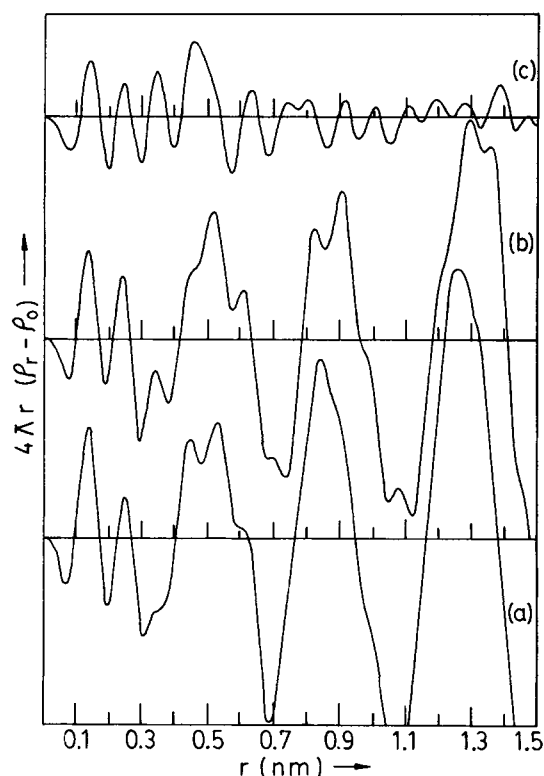


Figure 4 Differential radial distribution function curves for heat-treated ramie: (a) untreated, (b) 250°C, and (c) 300°C.

above may result from the loss of crystallinity, chain scission, dehydration, and auto-crosslinking. The well-resolved small peaks beyond $r > 0.6$ nm indicate the increased amorphous content in the sample. However, the presence of practically all the peaks even in almost fully amorphous sample (heat-treated at 300°C) indicates the presence of some amount of residual order in the packing of neighboring sections of chain molecules.

Table II Peak Positions (PP), Coordination Number (CN), Mean Square Displacement (\bar{u}^2), and Coupling Constant (CC) Values in Heat-Treated Ramie

Untreated				Heat-Treated at 250°C				Heat-Treated at 300°C			
PP (nm)	CN	$\bar{u}^2 \times 10^{-2}$ (nm ²)	CC	PP (nm)	CN	$\bar{u}^2 \times 10^{-2}$ (nm ²)	CC	PP (nm)	CN	$\bar{u}^2 \times 10^{-2}$ (nm ²)	CC
0.14	3.5	0.06	0.34	0.14	2.9	0.06	0.29	0.14	2.0	0.05	0.24
0.25	5.9	0.10	0.42	0.24	6.0	0.10	0.37	0.24	5.4	0.10	0.35
0.30	2.1	0.03	0.22	0.31	2.8	0.04	0.23	0.30	1.9	0.04	0.22
0.36	7.8	0.09	0.42	0.35	8.3	0.10	0.37	0.35	10.7	0.12	0.36
0.46	21.7	0.38	0.83	0.46	24.7	0.42	0.76	0.45	11.9	0.53	0.78
0.53	27.6	0.53	0.98	0.53	22.9	0.56	0.88	0.51	25.3	0.53	0.78

CONCLUSIONS

The present study shows that the RDF analysis of semicrystalline ramie fibers reveals useful information regarding the organizational arrangement of macromolecules in the fiber, although the interpretation is not straightforward for such a nonideal complex system. The results indicate a difference in both the conformation and the packing arrangement of molecular chains in raw and mercerized ramie. The coupling constant values associated with the interatomic vectors are in general observed to be higher in the alkali-treated fibers indicating relatively weak bond strength and diminished cohesion than that in untreated fibers. The effect of secondary valence force, such as van der Waals forces and hydrogen bonds, are apparent for $r > 0.2$ nm in the RDF curve. The region 0.3–0.6 nm of the DRDF curve appears to be more sensitive to the change in conformation and packing arrangement of chains, and at higher r values the interchain scattering predominates.

In the heat-treated ramie at 250 and 300°C, respectively, in general a marginal decrease in the coupling constant values is observed compared to the untreated sample. Some residual order in the packing of neighboring chain segments seems to exist even in the sample heat-treated at 300°C.

One of us (K.P.S) is grateful to Director, JTRL (ICAR), for kindly sponsoring him during this work.

REFERENCES

1. P. H. Hermans, *Physics and Chemistry of Cellulose Fibers*, Elsevier, Amsterdam, 1949.
2. H. P. Klug and L. E. Alexander, *X-Ray Diffraction Procedure for Polycrystalline and Amorphous Materials*, 2nd ed., Wiley, New York, 1974.
3. H. Bjornhaug, O. Ellefsen, and B. A. Tonnesen, *Norsk Skogind.*, **7**, 171 (1953).
4. H. Bjornhaug, O. Ellefsen, and B. A. Tonnesen, *J. Polym. Sci.*, **12**, 621 (1954).
5. O. Ellefsen, E. W. Lund, B. A. Tonnesen, and K. Oien, *Norsk Skogind.*, **11**, 284 (1957).
6. O. Ellefsen, K. Kringstad, and B. A. Tonnesen, *Norsk Skogind.*, **18**, 419 (1964).
7. A. N. J. Heyn, *J. Appl. Phys.*, **26**, 1113 (1955).
8. N. Norman, *Text. Res. J.*, **33**, 711 (1963).
9. T. Petitpas, M. Oberlin, and J. Mering, *J. Polym. Sci.*, **C2**, 423 (1963).
10. H. P. Fink, B. Phillip, D. Paul, R. Serimaa, and T. Paakkari, *Polymer*, **28**, 1265 (1987).
11. T. P. Nevell and S. H. Zeronian, Eds., *Cellulose Chemistry and Applications*, Wiley, New York, 1985.
12. K. P. Sao, M. D. Mathew, and P. K. Ray, *Text. Res. J.*, **57**, 407 (1987).
13. J. O. Warwicker, in *Cellulose and Cellulose Derivatives, Part IV*, N. M. Bikales and L. Segal, Eds., Wiley-Interscience, New York, 1971, p. 354.
14. T. Okano and A. Sarko, *J. Appl. Polym. Sci.*, **30**, 325 (1985).
15. R. F. Kruh, in *Handbook of X-Rays*, E. F. Kaelble, Ed., McGraw-Hill, New York, 1967, Chap. 22.
16. D. T. Cromer and J. T. Weber, *Acta Cryst.*, **18**, 104 (1965).
17. F. Hajdu, *Acta Cryst.*, **A27**, 73 (1971).
18. J. Krough-Moe, *Acta Cryst.*, **9**, 951 (1956).
19. B. E. Warren, *X-Ray Diffraction*, Adison-Wesely, Reading, MA, 1969, p. 116.
20. R. Kaplow, A. Rowe, and B. L. Averbach, *Phys. Rev.*, **168**, 1068 (1968).
21. H. Morimoto, *J. Phys. Soc. (Jpn.)*, **13**, 1015 (1958).
22. K. P. Sao, Ph.D. Thesis, I. I. T. Kharagpur, India (1991).
23. C. S. Wang and G. S. Y. Yeh, *J. Macromol. Sci.-Phys.*, **B15**(1), 107 (1978).
24. S. Arnott and W. E. Scott, *J. Chem. Soc. Perkin Trans.*, **2**, 324 (1972).
25. E. Ott, H. M. Spurlin, and M. W. Grafflin, Eds., *Cellulose and Cellulose Derivatives, Part I*, Interscience, New York, 1954.
26. J. O. Warwicker and A. C. Wright, *J. Appl. Polym. Sci.*, **11**, 659 (1967).
27. F. Hajdu, *Phys. Stat. Sol.*, **60**, 365 (1980).
28. K. H. Gardner and J. Blackwell, *Biopolymers*, **13**, 1975 (1974).
29. R. H. Attala, *Appl. Polym. Symp.*, **28**, 659 (1976).
30. A. Sarko, *Appl. Polym. Symp.*, **28**, 729 (1976).
31. B. Philipp, H. P. Fink, J. Kunze, and K. Frigge, *Ann. Physik Leipzig*, **42**, 507 (1985).
32. E. Back, M. T. Htun, M. Jackson, and F. Johanson, *Tappi*, **50**, 542 (1967).
33. H. Hatakeyama, T. Hatakeyama, and J. Nakano, *Appl. Polym. Symp.*, **28**, 743 (1976).

Accepted August 20, 1993

Received January 12, 1994